American Mineralogist, Volume 73, pages 982–992, 1988

Crystal-growth kinetics of plagioclase in igneous systems: Isothermal H_2O-saturated experiments and extension of a growth model to complex silicate melts

GREGORY E. MUNCILL
Geophysical Laboratory, 2801 Upton Street N.W., Washington, D.C. 20008, U.S.A.
ANTONIO C. LASAGA
Department of Geology and Geophysics, Yale University, New Haven, Connecticut 06511, U.S.A.

ABSTRACT

Crystal-growth rates have been experimentally determined for the growth of plagioclase from melts in the H_2O-saturated system $NaAlSi_3O_8$-$CaAl_2Si_2O_8$-H_2O (Ab-An-H_2O). As in an earlier study on crystal growth rates for plagioclase crystal growth in the 1-atm Ab-An system (Muncill and Lasaga, 1987), we have developed an extension of simple, single-component growth theory to predict crystal-growth rates. Unlike the earlier study, the predicted growth rates vary considerably from the experimentally derived growth rates, probably as a result of errors in the calculated viscosities for the experimental bulk compositions or because of a failure of the Stokes-Einstein equation relating diffusion rates and viscosities.

The combination of the observed growth rates and data on compositions of the crystals and glasses can be used to constrain the possible mechanisms of crystal growth within the Ab-An-H_2O system. The rate-controlling factor at low undercoolings is the reaction at the crystal-melt interface. At low and moderate undercoolings the resulting crystals are essentially unzoned and reflect the equilibrium compositions for the growth temperature. The growth mechanism at low and moderate undercoolings appears to represent a coupling of advective and diffusive mass transfer in controlling the growth rate.

INTRODUCTION

The field of geochemistry has undergone rapid evolutionary changes over the past two to three decades with the development of an expanding thermodynamic database and the application of equilibrium thermodynamic principles to natural systems. The success of the method can be measured by the additional constraints that can be placed on thermodynamic variables, such as pressure, temperature, and phase assemblages through the application of equilibrium thermodynamics.

Geochemists have become increasingly aware, however, that an even greater amount of information can be unlocked from evaluation of the kinetic or time-dependent pathways that a natural system follows. In many instances, traces of the kinetic pathway can be found through measurement of "frozen-in" disequilibrium within the natural system. Geochemical kinetics, unlike equilibrium thermodynamics, will provide constraints on the physicochemical evolution of natural systems through time.

The present study was initiated with the intent of developing the experimental and theoretical techniques to be able to deduce the kinetic pathway of igneous minerals with "frozen-in" disequilibrium compositional zoning. A rock-forming mineral phase that can display complex compositional zoning is plagioclase feldspar. In order to model the crystallization pathway of this mineral phase, we must first investigate experimentally the kinetics of the crystal-growth process. The growth-rate data can be used to explore the possible growth models. The resulting crystal-growth models can be used to investigate the possible modes of origin of the complex compositional zoning observed in natural igneous plagioclase.

An experimental study on crystal-growth kinetics in the H_2O-saturated $NaAlSi_3O_8$-$CaAl_2Si_2O_8$-H_2O (Ab-An-H_2O) system represents a natural extension of the 1-atm study of Muncill and Lasaga (1987). The previous study provided detailed information on crystal growth of plagioclase in the anhydrous Ab-An system. In addition, the growth data could be described by an extension of simple, single-component growth theory to multicomponent systems. The primary impetus of the present study was twofold; we were interested in collecting crystal-growth data at elevated pressures as a comparison to our previous work with the binary, 1-atm system, and we wanted to explore the applicability of our simple growth model to more complex systems.

EXPERIMENTAL PROCEDURE

Preparation of starting materials

The compositions of the anhydrous starting materials correspond to crystalline plagioclase compositions of An_{30} and An_{10}

0003–004X/88/0910–0982$02.00

(mol%). The starting materials consisted of the same anhydrous, fired gels as used by Muncill and Lasaga (1987). Seed crystals of natural anorthite (An_{97}) were used to avoid the added variable of lag time from homogeneous nucleation. Seed crystals of uniform size (100–250 μm) were prepared from crystals of natural, igneous anorthite by grinding and sieving. A complete description of the preparation procedure, wet-chemical analyses of the starting materials, and an average composition of the anorthite from several electron-microprobe analyses can be found in our earlier paper.

Crystal-growth experiments

H_2O-saturated crystal-growth experiments were carried out at 2 and 5 kbar in an internally heated pressure vessel (IHPV). The experimental apparatus has been previously described in detail by Holloway (1971). A detailed study was carried out at 2 kbar for growth in the H_2O-saturated An_{10} and An_{30} systems. Although a detailed growth curve was determined for crystal growth in the An_{10} system at 5 kbar, only two survey points were determined for the An_{30} system at 5 kbar.

Pressure was generated using single-stage and two-stage intensification (2 and 5 kbar, respectively) with Ar as the pressure medium. The pressure was measured with a manganin cell calibrated against a Heise Bourdon-tube gauge and is believed to be accurate to within ± 100 bars. The furnace for the IHPV consisted of two semi-independent $Pt_{90}Rh_{10}$ windings around a high-density grooved alumina tube. The furnace was controlled by a solid-state proportional controller, and temperatures were measured with two bare-wire Pt-$Pt_{90}Rh_{10}$ thermocouples. The thermocouples were calibrated in situ against the melting point of Au (1063.5 °C) at 1 atm. No pressure correction was made for the thermocouple readings, and recorded run temperatures are believed to be accurate to within ± 5 °C. The capsule(s) for each experiment were placed between the two thermocouples, and temperature gradients between the two thermocouples could be restricted to 0–2 °C.

The anhydrous starting material consisted of a mixture of 100–200 mg of the appropriate starting composition and 1–2 mg of anorthite seed crystals. The anhydrous mix and triply distilled H_2O were placed into a 5-mm–outside diameter Pt capsule that had been welded shut at one end. The capsules were sealed, weighed, and placed in a 120 °C oven overnight in order to aid homogenization of water distribution within the capsule and to check for leaks. The capsules were subsequently reweighed, and any capsules that had lost weight were discarded. One or two capsules per run were placed in the IHPV, and pressure was increased to an intermediate value (1 kbar for the 2-kbar runs and 2.5 kbar for the 5-kbar runs). Temperature was then brought up slowly over the course of 2–4 h to a temperature either 50 °C (An_{30}) or 85–100 °C (An_{10}) above the liquidus for the particular bulk composition and pressure. The pressure, because of expansion of the Ar with temperature, would be close to the run pressure. The pressure was then adjusted to the appropriate pressure for the experiment. The liquidus temperatures for the H_2O-saturated Ab-An-H_2O system at 2 and 5 kbar have been previously determined experimentally (Yoder et al., 1957; Erikson, 1979). The liquidus temperatures could also be checked by the results of the growth experiments, i.e., growth or absence of growth. The experiments were maintained at a hyperliquidus temperature for 1½ h (An_{30}) to 7 h (An_{10}). The length of the chosen homogenization time was important, because longer homogenization times resulted in complete dissolution of the seed crystals and shorter homogenization times resulted in incomplete conversion of the bulk starting material into a hydrous melt phase.

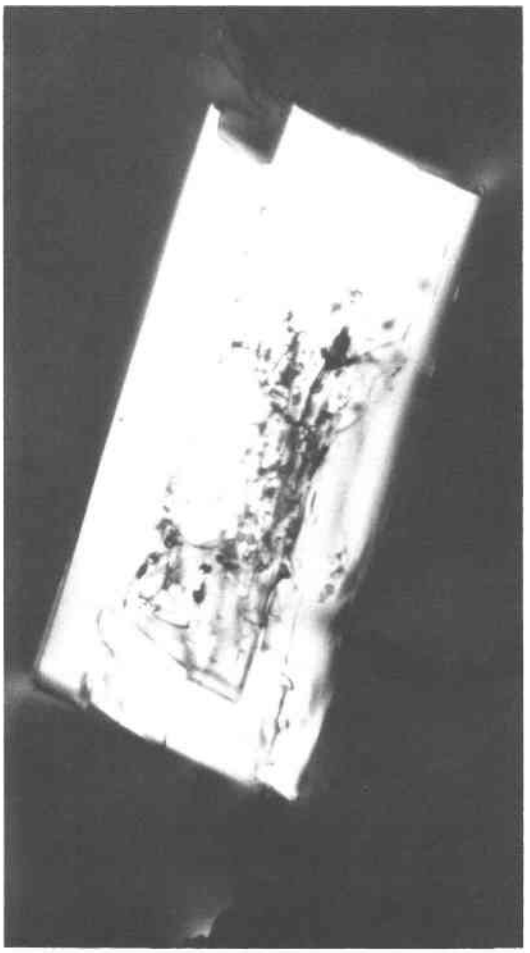

Fig. 1. Photomicrograph of crystal morphology with crossed polarizers showing tabular crystal growth around a seed crystal. The field of view is 0.8 mm. $\Delta T = 30$ °C; bulk composition = An_{10}.

After homogenization was complete, the temperature was quickly dropped to the particular temperature of interest. Generally, the temperature would undershoot the set temperature by 5–10 °C, but would stabilize at the set temperature within 5–8 min. Pressure was then adjusted to the particular pressure for the experiment, either 2 or 5 kbar. After a predetermined length of time, the experiment was quenched isobarically, which resulted in cooling to subsolidus temperatures within approximately 3 min.

The capsules were weighed after an experiment to insure that they had not leaked. The capsules were then opened, and the resulting run products were observed to consist of a glass slug with imbedded crystals and free water. The glass slug was mounted in epoxy, and a polished thin section was prepared for optical and electron-microprobe analysis.

Experimental results

Crystal morphology

For the 2-kbar experiments with the An_{30} composition, there was a progressive change of crystal morphology with

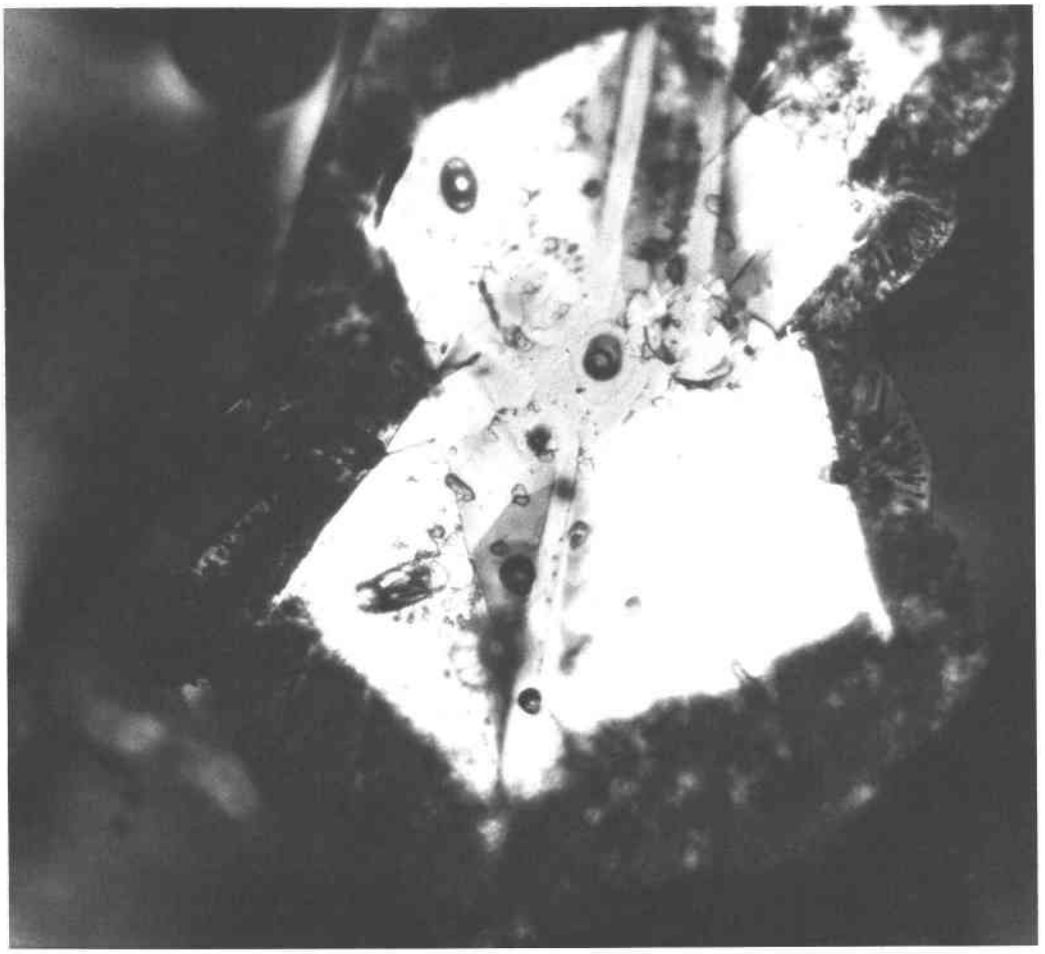

Fig. 2. Photomicrograph of crystal morphology for tabular crystal growth from homogeneous nucleation (crossed polarizers). Note the thin, crosscutting platelets. Field of view is 0.8 mm. ΔT = 18 °C; bulk composition = An_{30}.

undercooling that was similar to the 1-atm experiments of Muncill and Lasaga (1987) and to previous IHPV studies (Lofgren, 1974). For undercoolings of less than 40 °C, the crystals are predominately tabular. The crystals that nucleate heterogeneously on the anorthite seed crystals occur as relatively thick tabular crystals, with an average *a*:*c*:*b* ratio of approximately 10:10:1 (Fig. 1). Conversely, crystals that nucleate homogeneously occur as relatively thin platelets with an average *a*:*c*:*b* ratio of approximately 20:20:1 (Fig. 2).

At undercoolings between 40 and 100 °C, the crystals principally occur as skeletal crystals with average *a*:*c*:*b* ratios within the range of 25:5:1 (lower undercoolings) to 40:5:1 (higher undercoolings). Again, consistent with previous studies (Muncill and Lasaga, 1987; Fenn, 1977; Swanson, 1977), the principal growth direction is along the *a* crystallographic axis.

At undercoolings of 100 to 200 °C, the plagioclase morphology can be described as fibrilar, with the formation of bundles of acicular crystals. At undercoolings greater than 200 °C, the plagioclase grows as spherulitic crystals, which form radial patterns around the anorthite seed crystals. There were no observations of dendritic growth, which presumably could occur somewhere in the 100 to 200 °C range of undercooling.

The variations in crystal morphology of the plagioclase in the 2-kbar growth experiments with the An_{10} bulk composition generally resemble the variations from the An_{30} experiments with only a few differences. The respective ranges for the appearance of each crystal morphology are nearly identical, except that the range of the lath or skeletal morphology is at 40 to 110 °C undercooling. In addition, within this 40 to 110 °C undercooling range, the morphology of the crystals is more akin to lath-shaped crystals than the skeletal form of the crystals.

When viewed with the aid of a petrographic microscope, the crystals from the 2-kbar experiments with the An_{10} and An_{30} bulk compositions do not appear to be compositionally zoned, because the extinction angles for the crystals do not vary under crossed polars; this is similar to the results of the 1-atm experiments. As in the 1-atm experiments, the crystals also form growth twins during growth at low to moderate undercoolings (20–110 °C).

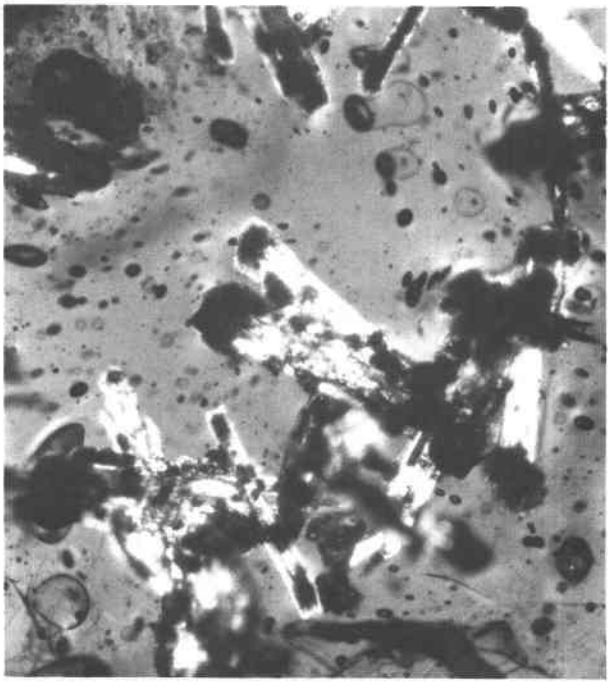

Fig. 3. Photomicrograph showing development of fluid-inclusion "halos" around the elongate ends of crystals. The run is viewed under partially crossed polarizers. The field of view is 3.2 mm. $\Delta T = 41$ °C; bulk composition = An_{30}.

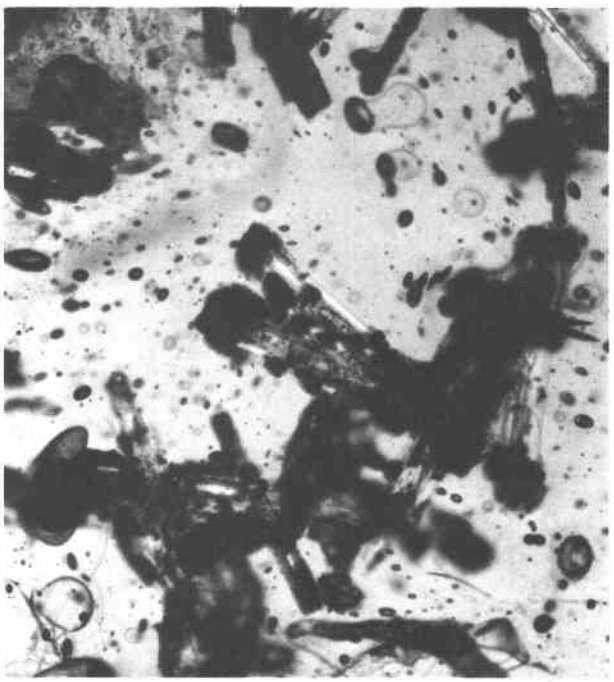

Fig. 4. The same view as in Fig. 3, but with polarizers uncrossed.

Another feature that is observed at undercoolings greater than 20 to 40 °C is the formation of vesiculated glass "halos" around the elongate ends of the plagioclase crystals (see Figs. 3 and 4). This phenomenon is believed to represent quenched melt plus fluid-filled bubbles that existed next to the crystal face during growth.

The temperature range for the appearance of each successive growth morphology in the 5-kbar experiments with the An_{10} bulk composition is significantly expanded in comparison to the 2-kbar experiments. The euhedral tabular morphology for the plagioclase crystals is predominant over an undercooling range of at least 0 to 110 °C. At an undercooling of 170 °C, the plagioclase crystals occur as lath-shaped crystals, and at an undercooling of 270 °C, the plagioclase grows as radial spherulitic aggregates around the anorthite seed crystals. Thus, the field of euhedral tabular growth is expanded from 0–40 °C to greater than 0–110 °C undercooling with the increase in pressure from 2 to 5 kbar and the concomitant increase in H_2O content of the melt. The expansion of the temperature range for each distinctive crystal morphology has been previously observed by Lofgren (1974) for plagioclase growth from H_2O-saturated plagioclase melts at 6 kbar. In Lofgren's study, however, he did not report any lath-shaped crystals growing from the An_{10} bulk composition at 6 kbar. As in the 2-kbar experiments, there is the formation of vesiculation "halos" around the elongate ends of the crystals at moderate (greater than 60 °C) undercoolings. The crystals also form growth twins over a wider range of undercooling (0 to greater than 170 °C) than in the 2-kbar experiments.

Crystal-growth rates

Figure 5 represents the growth-rate data for An_{10} and An_{30} bulk compositions under H_2O-saturated conditions at 2-kbar confining pressure as a function of temperature. Figure 6 presents similar data for the An_{10} composition at 5 kbar and two survey growth temperatures for the An_{30} bulk composition. Growth-rate curves have been hand-fitted to the maxima for the growth rates as a function of undercooling.

As can be seen from the figures, the growth-rate curves increase rapidly with undercooling below the liquidus temperature, reach a maximum, and then decrease slowly with relatively large undercoolings. The appearance of a maximum in growth rate is a common feature of crystal growth from glass-forming systems (Winkler, 1947; Jackson, 1967; Kirkpatrick et al., 1979). In comparison to the 1-atm experiments of Muncill and Lasaga (1987), however, the curves for growth from H_2O-saturated plagioclase melts have much broader maxima; the decrease in growth rates at large undercoolings is not as great as with the 1-atm experiments. This phenomenon may result from the enhanced diffusivity of the growth species in the H_2O-saturated plagioclase melts over that in the anhydrous melts.

The growth rates can be compared with the growth rates reported by Fenn (1977) for growth of alkali feldspar in H_2O-bearing albite-orthoclase melts at 2.5 kbar. The maximum growth rate for the An_{10} melt is approximately

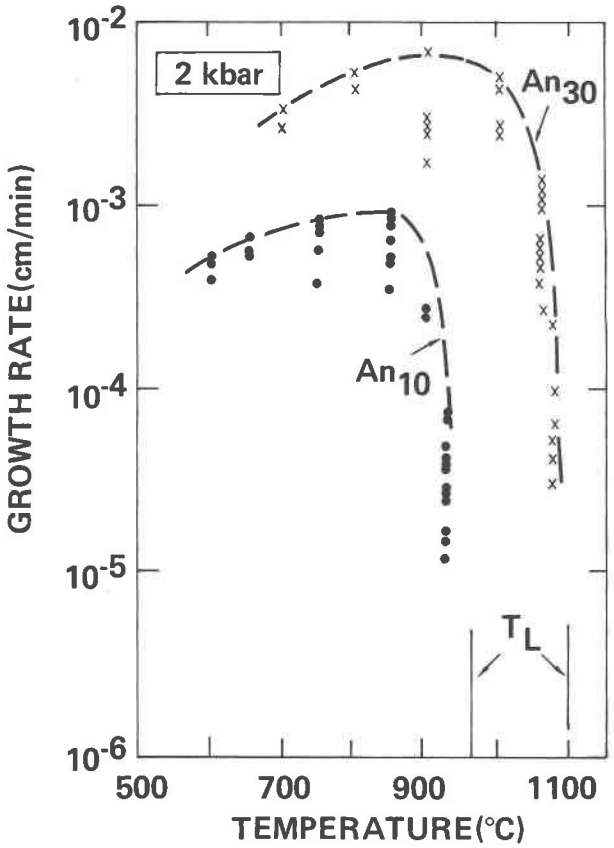

Fig. 5. Experimental growth rates for 2-kbar H_2O-saturated experiments plotted versus temperature.

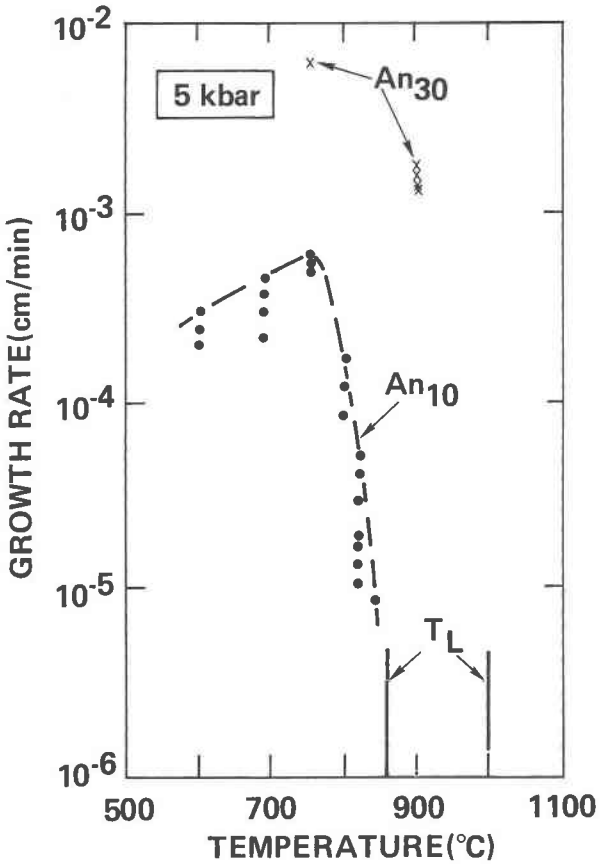

Fig. 6. Experimental growth rates for 5-kbar H_2O-saturated experiments plotted versus temperature. Two survey experiments for An_{30} bulk composition are presented along with the An_{10} data.

50% to 80% greater than the maxima found by Fenn. The growth-rate maximum for the An_{30} bulk composition is slightly over an order of magnitude greater than the maxima reported by Fenn.

Discussion

Extension of basic theory

In our earlier study (Muncill and Lasaga, 1987) we derived a simplified growth expression for crystal growth in the 1-atm plagioclase system. The theory is based on data for single-component crystal growth. The form of the equation is

$$Y_{Pl} = [1 - \exp(-\Delta H_m \Delta T/RTT_L)]Y_r/\eta, \quad (1)$$

where Y_{Pl} = growth rate of plagioclase at 1 atm (cm/s), ΔH_m = enthalpy of melting (J/mol), R = gas constant [J/(K·mol)], T = temperature of growth (K), T_L = liquidus temperature of the crystalline phase (K), $\Delta T = T_L - T$ (K), Y_r = reduced growth rate [cm·poise/(s·K)], and η = viscosity of the melt phase (poise).

In Muncill and Lasaga (1987), Y_r was derived from crystal-growth data of the pure anorthite end member. The equation was then successfully used to model crystal-growth rates across the 1-atm plagioclase binary. If the nature of the hydrous crystal-melt interface is not too different from that of the anhydrous crystal-melt interface, the reduced growth rate, Y_r, should have the same functional form for growth in both the anhydrous and hydrous plagioclase melts. For the case of growth from a hydrous melt, Equation 1 is now of the form

$$Y_{Pl} = [1 - \exp(-\Delta H_{hm,An_q} \Delta T/RTT_L)]Y_r/\eta, \quad (2)$$

where all of the variables are as previously defined for Equation 1, with the exception of $\Delta H_{hm,An_q}$, which is the enthalpy of melting for a plagioclase of composition q in a hydrous melt. For the present purposes, we will be interested in the enthalpy of melting of plagioclase in H_2O-saturated plagioclase melts at 2- and 5-kbar pressure. The appropriate reaction for crystallization of 1 mol of H_2O-saturated plagioclase melt is

$$An_{hm,c} \rightarrow yAn_{hm,0} + (1 - y)An_{s,q} + (1 - y)n_w H_2O_v, \quad (3)$$

where $An_{hm,c}$ = H_2O-saturated plagioclase melt of composition c, $An_{hm,0}$ = H_2O-saturated plagioclase melt of composition 0 (pure H_2O-saturated albite melt), $An_{s,q}$ = solid plagioclase of composition q, n_w = moles of H_2O in hydrous melt per mole of anhydrous melt, hm = hydrous melt (H_2O-saturated), and v = vapor.

The enthalpy of the melting reaction, which is simply the opposite of Reaction 3, is given by

$$\Delta H_{\mathrm{hm,An}_q} = \bar{H}_{\mathrm{hm,An}_c} - y\bar{H}_{\mathrm{hm,Ab}} - (1 - y)\bar{H}_{\mathrm{s,An}_q} - (1 - y)n_w\bar{H}_{\mathrm{v,w}}, \quad (4)$$

where $\Delta H_{\mathrm{hm,An}_q}$ = enthalpy of hydrous (H_2O-saturated) melting of $1 - y$ moles of plagioclase of composition q, $\bar{H}_{z,x}$ = partial molar enthalpy of phase z of composition x, and $\bar{H}_{\mathrm{v,w}}$ = molar enthalpy of H_2O vapor at P and T. If we further assume ideal mixing in the solid and melt phases, we have

$$\bar{H}_{\mathrm{s,An}_q} = q\bar{H}_{\mathrm{s,An}} + (1 - q)\bar{H}_{\mathrm{s,Ab}} \quad (5)$$

and

$$\bar{H}_{\mathrm{hm,An}_c} = c\bar{H}_{\mathrm{hm,An}} + (1 - c)\bar{H}_{\mathrm{hm,Ab}}. \quad (6)$$

where $\bar{H}_{\mathrm{s},z}$ = molar enthalpy of solid z at P and T and $\bar{H}_{\mathrm{hm},z}$ = partial molar enthalpy of z in the hydrous melt at P and T.

Substitution of Equations 5 and 6 into Equation 4 results in

$$\Delta H_{\mathrm{hm,An}_q} = c\bar{H}_{\mathrm{hm,An}} + (1 - c)\bar{H}_{\mathrm{hm,Ab}} - y\bar{H}_{\mathrm{hm,Ab}} - (1 - y)[qH_{\mathrm{s,An}} + (1 - q)H_{\mathrm{s,Ab}}] - (1 - y)n_wH_{\mathrm{v,w}}. \quad (7)$$

From mass-balance considerations, it follows that

$$c = y \cdot 0 + (1 - y)q, \quad (8)$$

which can be rearranged as

$$y = (q - c)/q. \quad (9)$$

Substitution for c in Equation 7 from Equation 9 yields

$$\Delta H_{\mathrm{hm,An}_q} = (1 - y)q(\bar{H}_{\mathrm{hm,An}} - \bar{H}_{\mathrm{s,An}}) + (1 - y)(1 - q)(\bar{H}_{\mathrm{hm,Ab}} - \bar{H}_{\mathrm{s,Ab}}) - (1 - y)n_w\bar{H}_{\mathrm{v,w}}. \quad (10)$$

The last term can be rewritten as

$$(1 - y)n_w\bar{H}_{\mathrm{v,w}} = n_w(1 - y)[q\bar{H}_{\mathrm{v,w}} + (1 - q)\bar{H}_{\mathrm{v,w}}],$$

which can be substituted into Equation 10 with the result

$$\Delta H_{\mathrm{hm,An}_q} = (1 - y)q(\bar{H}_{\mathrm{hm,An}} - \bar{H}_{\mathrm{s,An}} - n_w\bar{H}_{\mathrm{v,w}}) + (1 - y)(1 - q)(\bar{H}_{\mathrm{hm,Ab}} - \bar{H}_{\mathrm{s,Ab}} - n_w\bar{H}_{\mathrm{v,w}}). \quad (11)$$

Equation 11 can be rewritten as

$$\Delta H_{\mathrm{hm,An}_q} = (1 - y)q\Delta H_{\mathrm{hm,An}} + (1 - y)(1 - q)\Delta H_{\mathrm{hm,Ab}},$$

or

$$\Delta H_{\mathrm{hm,An}_q} = (1 - y)[q\Delta H_{\mathrm{hm,An}} + (1 - q)\Delta H_{\mathrm{hm,Ab}}]. \quad (12)$$

If local equilibrium is assumed to prevail between the crystal and melt phase, we have

$$K = q/c, \quad (13)$$

where K is the Nernst equilibrium partition coefficient. If Equation 13 is used to substitute for y and q in Equation 12, the resulting equation is

$$\Delta H_{\mathrm{hm,An}_q} = c\Delta H_{\mathrm{hm,An}} + [(1 - Kc)/K]\Delta H_{\mathrm{hm,Ab}}. \quad (14)$$

The form of Equation 14 is similar to the formulation developed by us for the binary system Ab-An (Eq. 1), except that Eq. 14 now involves enthalpies of H_2O-saturated melting for anorthite and albite at pressure, rather than the enthalpies of melting in the 1-atm, anhydrous system. In order to calculate crystal-growth rates in H_2O-saturated plagioclase melts, we now need to determine the enthalpies of H_2O-saturated melting for albite and anorthite for our two sets of experimental conditions. For the present study, the enthalpies of H_2O-saturated melting of albite and anorthite were calculated according to the formulated equations of Burnham and Nekvasil (1986). The calculated $\Delta H_{\mathrm{hm,Ab}}$ values are 56 kJ/mol at 2 kbar (T_m = 1120 K) and 62 kJ/mol at 5 kbar (T_m = 1025 K); the corresponding $\Delta H_{\mathrm{hm,An}}$ values are 117 kJ/mol (2 kbar, 1600 K) and 116 kJ/mol (5 kbar, 1508 K). We will for now assume that the ΔH_{hm} values are independent of temperature. The effect of temperature-dependent ΔH_{hm} will be further evaluated later.

The required values for the viscosities of hydrous plagioclase melts can be calculated with the use of the empirical method of Shaw (1972). Although there may be some ambiguities in using the method to describe "simple" silicate melt systems (Shaw, 1972), the calculated curves fit most of the experimental data for hydrous melts. The only other required information is compositional and phase-equilibria data for the H_2O-saturated plagioclase system at 2- and 5-kbar confining pressure. Erikson (1979) has measured the appropriate 2-kbar data, and Yoder et al. (1957) have investigated the phase equilibria at 5 kbar.

We are now in a position to calculate rates for crystal growth in the H_2O-saturated system through the use of Equation 3. Figures 7 and 8 show the calculated versus experimental results for growth in H_2O-saturated melts at 2-kbar (An_{30} and An_{10}) and 5-kbar (An_{10}) pressure. Although the experimental and calculated curves for growth from the An_{10} melt at 2 kbar agree to within a factor of three, the agreement between the other curves is much less satisfactory. The calculated curve for growth in the 2-kbar H_2O-saturated An_{10} system now predicts growth rates that are too *large* by a factor of three; for growth in the anhydrous An_{10} system (Muncill and Lasaga, 1987), the calculated curve was a factor of seven to ten times *smaller* than the experimental curve. The worst fit is for growth in the H_2O-saturated An_{10} system at 5 kbar (Fig. 8), with a calculated curve 10 to 20 times larger than the experimental curve. Possible reasons for the observed discrepancy include (1) large temperature dependence of the entropies and enthalpies of melting, (2) a change in the mechanism for crystal growth in hydrous versus anhydrous plagioclase melts, (3) systematic errors in the fit of the viscosity data for hydrous plagioclase melts, and (4) failure of the Stokes-Einstein relationship to predict variations in diffusive transport of growth units in the hydrous melt system relative to the anhydrous system.

According to the formulation of Burnham and Nekvasil (1986), the temperature dependences of the entropy and enthalpy of melting for albite are relatively small in comparison to the absolute values. The values of $\Delta H_{\mathrm{hm,An}}$

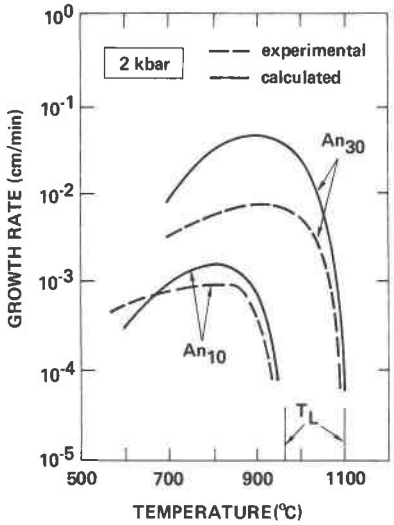

Fig. 7. Plot of calculated and experimental growth-rate curves as a function of temperature for 2-kbar H_2O-saturated experiments.

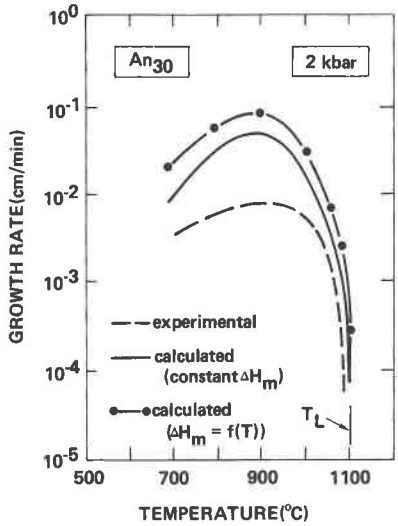

Fig. 9. Comparison of calculated growth-rate curves for a constant ΔH_{hm} and ΔH_{hm} as a function of temperature.

and $\Delta S_{hm,An}$, however, are more temperature dependent. The calculated values of $\Delta H_{hm,An}$ decrease linearly with decreasing temperature, with a slope of 63.5 J/K, whereas the values of $\Delta H_{hm,Ab}$ decrease linearly with a slope of 15.9 J/K. The effect of including the temperature dependence of $\Delta H_{hm,An}$ and $\Delta H_{hm,Ab}$ in the growth-rate equation is shown in Figure 9. The calculated growth-rate curve for the An_{30} bulk composition is shifted in the wrong direction. The shift in the growth-rate curve would be considerably less for the more albite-rich An_{10} composition. Although the temperature dependences of $\Delta H_{hm,An}$ and $\Delta H_{hm,Ab}$ do not appear to be responsible for the observed experimental versus calculated discrepancies, the effect could assume increasing importance in calculating growth rates in relatively anorthite-rich compositions.

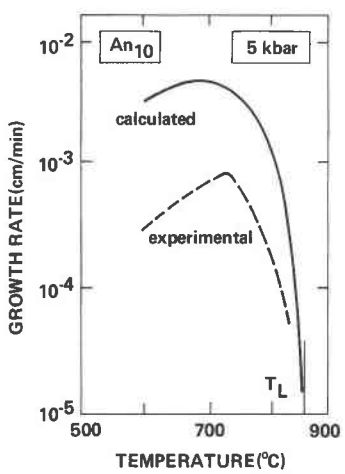

Fig. 8. Plot of calculated and experimental growth-rate curves as a function of temperature for growth in the H_2O-saturated An_{10} system at 5 kbar.

A change of growth mechanism would involve either a change in the attachment mechanism at the crystal-melt interface or a change in the transport process of growth units to the crystal-melt interface. In the case of a change in the attachment mechanism, we would expect a change in the structure and morphology of the crystal-melt interface; this change would be reflected in a change in the number of available growth sites as a function of temperature [$f(T)$]. The fraction of growth sites is one of the mixed set of terms represented by the reduced growth rate, Y_r. A change of growth mechanism could also arise from a change in the structural units that are involved in the attachment process at the crystal-melt interface. We can evaluate the relative change that would be expected for the fraction of growth sites [$f(T)$] in the transition from crystal growth in anhydrous to hydrous plagioclase melts. At the outset, however, we should note that Kirkpatrick et al. (1976) have shown that the closest fit between their data for growth of anorthite crystals from an anhydrous anorthite melt and very simple theoretical growth mechanisms involves some aspect of surface nucleation on the crystal surface (cf. Jackson, 1967). Of the possible surface-controlled growth reactions, surface-nucleation–controlled growth is the slowest. A change in mechanism for growth in hydrous plagioclase melts would require an even slower surface reaction in order to fit the observed data, which appears unlikely. The change in fraction of occupied surface sites for plagioclase crystals in anhydrous and hydrous melts can be evaluated according to a method devised by Jackson (1958, 1967) through the use of a factor, α, involving the entropy of melting:

$$\alpha = \Delta S_m \xi / R, \tag{15}$$

where ΔS_m = entropy of melting, ξ = fraction of total bonding energy represented by bonding parallel to the interface plane, and R = gas constant. For crystals with

α less than 2, the crystal-melt interface will be rough on the atomic scale; an example in silicate systems would be growth of cristobalite from a SiO_2 melt. Crystals with α greater than 2, such as plagioclase in a melt of plagioclase composition, will have crystal-melt interfaces that are smooth on the atomic scale.

The relative variations in the crystal-melt interface can be evaluated by calculating the ratio $\alpha_{2\text{kbar}}/\alpha_{1\text{atm}}$. The ξ term will be the same for both systems, because ξ is only a function of the structure of the crystal surface. The ξ term represents the fraction of total binding energy per atom in the plane of the crystal surface and will be independent of the media in which the crystal is growing. The relative change, in percent, of the fraction of occupied sites for crystals in the 2-kbar crystal-melt system versus the anhydrous system will be given by

$$\begin{aligned} F &= 100[(\alpha_{2\text{kbar}} - \alpha_{1\text{atm}})/(\alpha_{2\text{kbar}} + \alpha_{1\text{atm}})] \\ &= 100[(\Delta S_{\text{hm}} - \Delta S_{\text{m}})/(\Delta S_{\text{hm}} + \Delta S_{\text{m}})], \end{aligned} \quad (16)$$

where ΔS = entropy of anhydrous (m) melting at 1 atm or H_2O-saturated (hm) melting at 2 kbar.

If the calculation is performed for an An_{30} melt, entropies of melting at the liquidus temperature can be obtained from

$$\Delta S_{\text{m}} = \Delta H_{\text{m}}/T_{\text{L}}. \quad (17)$$

The corresponding values are 43.4 and 57.2 J/(mol·K) for $\Delta S_{\text{m,An}_{30}}$ and $\Delta S_{\text{hm,An}_{30}}$, respectively. The resulting value for F will then be +13.7%. The relatively low value is not too surprising, because Jackson (1967) has shown that for $\alpha \geq 2$, the crystal surface will always be smooth on an atomic scale; relatively small changes in α do not have a large effect on F. The relative change in the crystal-melt structure is clearly not of the magnitude required for the observed discrepancies between the calculated and observed growth rates in the An_{30} system.

A change in the mode of transport at the crystal-melt interface could result from a change in the growth species that are diffusing to the crystal surface, a change in the relative concentration of the growth species in the melt, or a combination of the two processes. In the transition from anhydrous to hydrous plagioclase growth, the melt becomes more depolymerized (Burnham, 1979a, 1981). One might expect that the relative radii of the growth units would then be less in hydrous melts than in anhydrous melts. If this assumption is true, however, the Stokes-Einstein relationship would predict a larger diffusion coefficient for mass transport for equivalent anhydrous and hydrous undercoolings (taking temperature differences into account). The growth rate should then *increase* for the hydrous melts in comparison with the anhydrous melts. If there is a change in the rate-controlling species, the species would have to be larger or possess a charge (which is not accounted for in the Stokes-Einstein relationship).

The experimental data indicate that there is a buildup of H_2O vapor around the faster-growing crystal faces of the plagioclase at moderate to large undercoolings in the 2- and 5-kbar experiments (see Figs. 3 and 4). The buildup of H_2O vapor at the crystal-melt interface has not been taken into account in the general growth Equation 2. The buildup of this "noncrystallizing" phase will further lower the concentration of growth units and lead to lower predicted growth rates. This mechanism will very likely be a contributing factor at moderate to large undercooling, but the "halo" phenomenon is not observed at low undercooling, where there are still significant discrepancies between experimental and calculated growth rates. Presumably, small concentration gradients in the H_2O content of the melt will result from the slow growth rate of the crystal at the low undercooling in comparison to the rate of diffusive transfer of the H_2O vapor through the melt.

The accuracy of the Shaw (1972) method for calculating viscosities of plagioclase hydrous melts cannot be evaluated because of a lack of experimental viscosity data for hydrous plagioclase melts. If errors in calculated viscosities of hydrous plagioclase melts are the cause of the observed discrepancies between calculated and observed growth rates, the calculated viscosities would have to be from a factor of 3 too low to 1½ orders of magnitude too low with no systematic variation in the error. Shaw's calculated curves, however, do fit most available experimental data for viscosities of hydrous "rock" melts to within a factor of +2 (see his Fig. 7). It would at first seem likely that Shaw's calculated viscosities for hydrous plagioclase melts could be in error by a factor of 3, but not by 1½ orders of magnitude. Shaw has cited a discrepancy between his empirical equation and published data on the viscosity of albite melt of approximately a factor of 7 (Shaw's value is a factor of 7 too small). Although the discrepancy is not sufficient to cause a 1½ order of magnitude change in the growth rate, it is in the right direction (the calculated viscosity underestimates the true viscosity). Clearly, additional viscosity data would be required to confirm the fit of Shaw's empirical equations.

If the calculated viscosities are valid, the discrepancies between calculated and experimental growth rates could be related to the assumption of a Stokes-Einstein relationship between mass transport and viscosity of the melts. A comparison of the growth-rate curve in Figure 5 with Figure 4 of Muncill and Lasaga (1987) shows that the curve for growth rates of plagioclase from H_2O-saturated An_{30} melt is within an order of magnitude of the corresponding growth curve in the anhydrous system. The variations in calculated viscosities between the anhydrous and hydrous melts, however, are approximately 2 to 2½ orders of magnitude at comparable degrees of undercooling, ΔT (*not* equivalent temperatures). Thus, the diffusion coefficient for the elementary growth unit, as calculated from the Stokes-Einstein relationship, should increase by 2 to 2½ orders of magnitude in the H_2O-saturated An_{30} melt in comparison to the anhydrous An_{30} melt. The result should be a relatively large increase in growth rates for the hydrous versus anhydrous An_{30} melts. If the viscosities are not in error, the experimental rate

TABLE 1. Coefficient values for the $f(\Delta T)$ polynomial

n	Value	n	Value
1	$2.873\,005\,353 \times 10^{-6}$	5	$-8.404\,426\,923 \times 10^{-12}$
2	$1.662\,208\,4 \times 10^{-5}$	6	$2.293\,550\,879 \times 10^{-14}$
3	$-2.298\,128\,538 \times 10^{-7}$	7	$-3.454\,616\,431 \times 10^{-17}$
4	$1.845\,564\,928 \times 10^{-9}$	8	$2.297\,638\,352 \times 10^{-20}$

data would not support the extension of the anhydrous Stokes-Einstein relationship—which is "normalized" to diffusive transport in anhydrous anorthite melt—to hydrous plagioclase melts.

We have considered the possible errors in viscosity and the Stokes-Einstein assumption as two end-member possibilities. Another, perhaps more likely explanation is that the discrepancies between the calculated and experimental growth rates are due to a combination of the two effects; confirmation of this idea would require, in addition to experimental viscosity data, data for diffusion coefficients in the anhydrous and hydrous plagioclase melts. Clearly, more experimental data are needed for comparisons of temperature-induced variations of vicosity and diffusion in silicate melt systems. One recourse is to treat the hydrous plagioclase melts in a manner similar to the anhydrous plagioclase melts: calculate a reduced growth rate for the "end member" An_{30} hydrous melt at 2-kbar P_{H_2O} and compare calculated growth rates for the H_2O-saturated An_{10} melt with the experimental curve. The new equation for growth in the hydrous system at 2-kbar P_{H_2O}, which is analogous to Equation 2, will be given by

$$Y_{Pl} = \left[1 - \exp\left(-\frac{\Delta H_{hm,An_9}\Delta T}{RTT_L}\right)\right] \cdot \frac{f(\Delta T)RT^2_{L,An_{30}(hm)}}{\Delta H_{hm,An_{30}}\eta}, \quad (18)$$

where $T_{L,An_{30}(hm)}$ = liquidus temperature for An_{30} H_2O-saturated bulk composition (1373 K), $\Delta H_{hm,An_{30}}$ = enthalpy of melting for An_{30} H_2O-saturated bulk composition, and $f(\Delta T)$ = polynomial in ΔT. The function $Y_{An_{30}}\eta/\Delta T$ was fit to a polynomial in ΔT as in our earlier study of growth in the anhydrous system. The resulting equation was solved as in the anhydrous case in order to derive Y'_r, the reduced growth rate, which was substituted into the growth equation. The resulting equation (18) is similar to the previous anhydrous and hydrous cases, except that now growth in the H_2O-saturated An_{30} bulk composition is the end-member case from which growth rates are calculated. The function $f(\Delta T)$ is given by

$$f(\Delta T) = \sum_{n=1}^{8} E_n \Delta T^n, \quad (19)$$

with the constants as given in Table 1.

Calculated and experimental curves for crystal growth in the H_2O-saturated An_{10} melt at 2 kbar are shown in Figure 10. The calculated curve now *underestimates* the experimental curve by a factor of 2 to 5. If the Shaw (1972) method consistently underestimates the viscosity

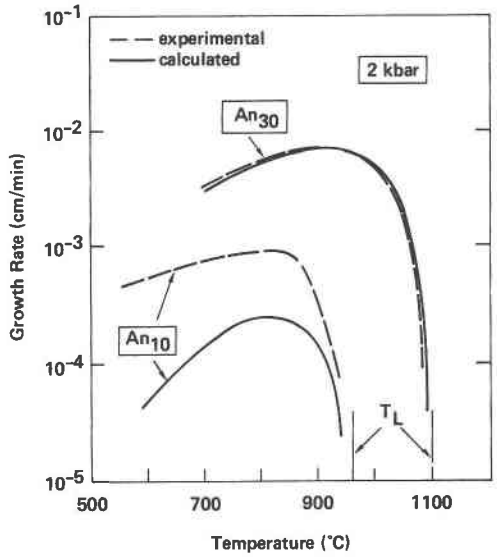

Fig. 10. Calculated and experimental growth-rate curves for An_{30} end-member case.

of hydrous melts upon addition of the anorthite component, we should observe a change from overestimation to underestimation of growth rates in the An_{10} system when "normalizing" the growth rate, as was observed.

For the present, the simplified growth model can be used to model crystal growth from anhydrous plagioclase melt compositions. Use of the model for calculation of crystal-growth rates from H_2O-saturated melts will require further experimental investigation of plagioclase growth rates in multicomponent systems and experimental evaluation of chemical diffusion rates in hydrous melts. Although interpolation to crystal growth in hydrous (not H_2O-saturated) plagioclase melts is tenuous, the variations in the maxima of the curves of growth rate versus undercooling between the H_2O-saturated (2 kbar) and anhydrous compositions are generally less than a factor of 2 (An_{10}) to 6 (An_{30}). Another feature is that the maxima for the growth-rate curve for the An_{10} composition pass through a maximum with increasing P_{H_2O}. The growth-rate maximum is an order of magnitude larger at 2-kbar P_{H_2O} in comparison to the 1-atm anhydrous case (Muncill and Lasaga, 1987), but the growth-rate maximum at 5-kbar P_{H_2O} is less than the maximum for growth at 2 kbar (see Figs. 5 and 6). Thus, it appears that the maxima of the growth rate curves for the An_{10} composition pass through a maximum as a function of P_{H_2O}. This observation of eventual decrease in growth rates as a function of increasing H_2O content of the melt is similar to the effect noted by Swanson (1977) for crystal growth in H_2O-saturated and H_2O-undersaturated synthetic granodiorite melts.

Compositions of crystals and glass (quenched melt)

Data on compositional zoning in the plagioclase crystals and analyses of concentration gradients in the glass

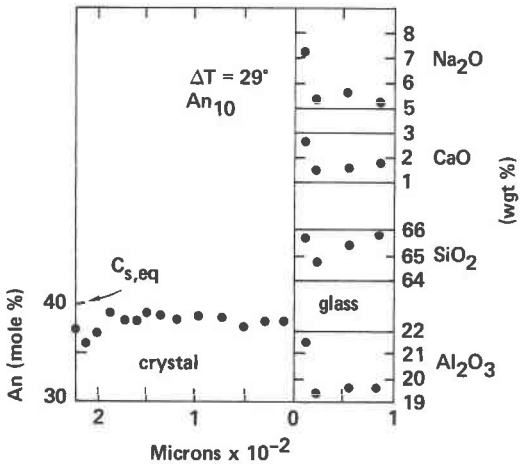

Fig. 11. Compositions of crystal and glass for run PT-21 at 2 kbar.

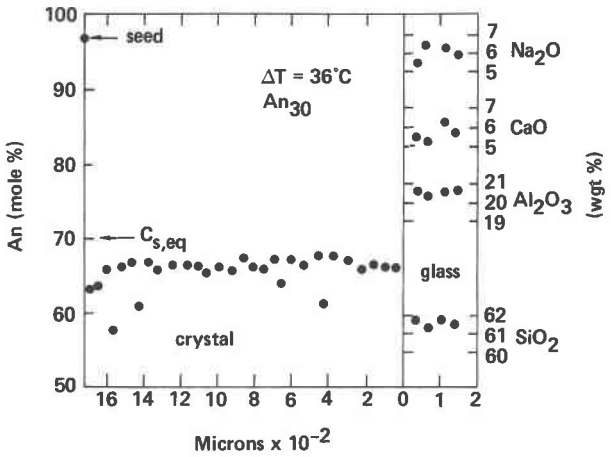

Fig. 12. Compositions of crystal and glass for run PT-27 at 2 kbar.

near the crystal-glass interface can provide further insights into the details of the growth process (Lasaga, 1981). In particular, compositional data can be used to evaluate the assumption of local equilibrium at the crystal-melt interface. In addition, compositional data on the crystal provide constraints on possible growth models that involve steady-state (Kirkpatrick et al., 1979; Lasaga, 1981) and non-steady-state conditions (Lasaga, 1982). Compositional data are provided in Figures 11 and 12 for crystals and glass in two of the H_2O-saturated 2-kbar experiments.

The compositions of the plagioclase crystals from the 2-kbar experiments correspond to the equilibrium compositions of the plagioclase crystals at the appropriate growth temperature (from data of Erikson, 1979). Similar correspondence between the plagioclase composition and the growth temperature was found for the 1-atm experiments of Muncill and Lasaga (1987). The crystals are generally compositionally unzoned, except for a curious reverse zoning near the center of the crystal. Compositions of the glasses next to the crystal faces in the 2-kbar experiments represent analyses over relatively large areas, as Na volatilization was a serious problem with a beam diameter of less than 40 μm. The amount of H_2O dissolved in the melts at 2 kbar is approximately 6 wt%, according to the model of Burnham (1979b), so representative totals for the hydrous glasses would be 98–99% when taking the H_2O into account. Within these analytical constraints, no apparent concentration gradients were detected in the glass next to the plagioclase crystals in the 2-kbar run products, as shown in the figures. The possibility should not be overlooked, however, that any existing concentration gradients could be significantly smaller ($\leq$40 μm) than the required minimum diameter of the electron beam of the microprobe.

Conclusions

Although the fit of simple theory to the experimental anhydrous growth curves is very satisfactory (Muncill and Lasaga, 1987), the multicomponent extension of simple theory provides a poor fit to the experimental growth-rate curves for H_2O-saturated crystal growth. Perhaps the most poorly constrained aspect of the extended model is the validity of the empirical viscosity equations of Shaw (1972) for simple hydrous melts. If the calculated values of viscosity are not in error, the most likely problem is with the assumption of a Stokes-Einstein relationship between diffusive mass transport and viscosity. Further evaluation will have to await new experimental viscosity data.

The details of the growth mechanism can be constrained in consideration of the multitude of growth models (Lasaga, 1981, 1982; Loomis, 1983). The rate-controlling step at low undercooling appears to be the reaction at the crystal-melt interface. Diffusive mass transport, with or without local equilibrium at the crystal-melt interface, is the most likely rate-controlling process at relatively large undercooling. At moderate undercooling, it is not clear whether the growth is controlled by a steady-state process or a slow approach to equilibrium. If the crystal-melt system was at steady state at moderate undercooling, however, the composition of the crystal was not the same as that of the melt, which would require advective mass transport in the melt in addition to the diffusive mass transfer (as a consequence of mass balance).

Important consequences arise when using the results to infer crystallization processes in natural systems. In the present isothermal experiments, there is no evidence of compositional zoning for the bulk of the plagioclase overgrowths surrounding the anorthite seed crystal. Although reverse zoning is observed in some instances in the plagioclase immediately surrounding the seed crystal (10 to 50 μm thick), the bulk of the crystal overgrowth is found to be unzoned. The compositions of the resulting crystals correspond to the equilibrium crystal composition for the particular growth temperature, regardless of the bulk composition. It appears that compositional zoning may only be induced by temperature and/or pressure varia-

tions in the bulk system with time. The effect of varying temperature with time during crystal growth has been investigated by one of us (Muncill, in prep.). In addition, at moderate undercoolings, the crystal-growth rate may be controlled by combined, diffusion-advection mass transfer to the crystal-melt interface. A diffusion-advection control on the growth process will require a re-evaluation of recent models based solely on diffusion through a stagnant melt as the process controlling the kinetics of the growth rate, such as Lasaga (1982) and Ghiorso (1987).

Acknowledgments

This research was supported in part by NSF grant no. EAR 80-0755 (to Lasaga). Portions of the study represent part of the Ph.D. thesis of Muncill at Penn State University. Muncill gratefully acknowledges support provided by an AMOCO Graduate Fellowship at Penn State University. Additional support was provided through the W. M. Keck Foundation Research Scholarship at the Geophysical Laboratory. Reviews on an earlier manuscript by Bjorn Mysen and Bob Luth are gratefully acknowledged. Critical and detailed reviews by James Kirkpatrick and Mark Ghiorso also helped to markedly improve the manuscript.

References cited

Burnham, C. Wayne (1979a) Magmas and hydrothermal fluids. In H.L. Barnes, Ed., Geochemistry of hydrothermal ore deposits. Wiley, New York.

——— (1979b) The importance of volatile constituents. In H.S. Yoder, Jr., Ed., The evolution of the igneous rocks. Princeton University Press, Princeton, New Jersey.

——— (1981) The nature of multicomponent aluminosilicate melts. In D.T. Rickard and F.E. Wickman, Eds., Chemistry and geochemistry of solutions at high temperatures and pressures: Physics and Chemistry of the Earth, 13–14, 197–229.

Burnham, C.W., and Nekvasil, H. (1986) Equilibrium properties of granite pegmatite magmas. American Mineralogist, 71, 239–263.

Erikson, R.L. (1979) An experimental and theoretical investigation of plagioclase melting relations. M.S. thesis, The Pennsylvania State University, University Park, Pennsylvania.

Fenn, P.M. (1977) The nucleation and growth of alkali feldspars from hydrous melts. Canadian Mineralogist, 15, 135–161.

Ghiorso, M.S. (1987) Chemical mass transfer in magmatic processes. III. Crystal growth, chemical diffusion and thermal diffusion in multicomponent silicate melts. Contributions to Mineralogy and Petrology, 96, 291–313.

Holloway, J.R. (1971) Internally heated pressure vessels. In G.C. Ulmer, Ed., Research techniques for high pressure and high temperature. Springer-Verlag, New York.

Jackson, K.A. (1958) Interface structure. In R.M. Doremus, B.W. Roberts, and D. Turnbull, Eds., Growth and perfection of crystals. Wiley, New York.

——— (1967) Current concepts in crystal growth from the melt. Progress in Solid State Chemistry, 4, 53–80.

Kirkpatrick, R.J., Robinson, G.R., and Hays, J.F. (1976) Crystal growth from silicate melts: Anorthite and diopside. Journal of Geophysical Research, 81, 5715–5720.

Kirkpatrick, R.J., Klein, L., Uhlmann, D.R., and Hays, J.F. (1979) Rates and processes of crystal growth in the system anorthite-albite. Journal of Geophysical Research, 84, 3671–3676.

Lasaga, A.C. (1981) Implications of a concentration-dependent growth rate on the boundary layer crystal-melt model. Earth and Planetary Science Letters, 56, 429–434.

——— (1982) Toward a master equation in crystal growth. American Journal of Science, 282, 1264–1288.

Lofgren, G. (1974) An experimental study of plagioclase crystal morphology: Isothermal crystallization. American Journal of Science, 274, 243–273.

Loomis, T.P. (1983) Compositional zoning of crystals: A record of growth and reaction history. In S.K. Saxena, Ed., Kinetics and equilibrium in mineral reactions. Springer-Verlag, New York.

Muncill, G.E., and Lasaga, A.C. (1987) Crystal-growth kinetics of plagioclase in igneous systems: One-atmosphere experiments and application of a simplified growth model. American Mineralogist, 72, 299–311.

Shaw, H.R. (1972) Viscosities of magmatic silicate liquids: An empirical method of prediction. American Journal of Science, 272, 870–893.

Swanson, S.E. (1977) Relation of nucleation and crystal-growth rate to the development of granitic textures. American Mineralogist, 62, 966–978.

Winkler, H.G.F. (1947) Kristallgrosse und Abkuhlung. Heidelberger Beitrage zur Mineralogie und Petrographie, 1, 251–268.

Yoder, H.S., Stewart, D.B., and Smith, J.R. (1957) Ternary feldspars. Carnegie Institution of Washington Year Book 56, 206–214.

Manuscript received March 3, 1987
Manuscript accepted May 6, 1988